JTTEE5 19:119–127
DOI: 10.1007/s11666-009-9381-7
1059-9630/$19.00 © ASM International

The Effect of Heat Treatment on the Oxidation Mechanism of Blended Powder Cr_3C_2-NiCr Coatings

S. Matthews, B. James, and M. Hyland

(Submitted April 16, 2009; in revised form July 21, 2009)

The advantageous oxidation and wear properties of Cr_3C_2-NiCr thermal spray coatings have resulted in them being extensively applied to combat erosion at high temperatures. Under these conditions, oxide layers take on an ever more significant role in determining the composite response. The response of blended powder-based carbide coatings for erosion applications has formed the basis for application of cermet-based coatings at elevated temperature. In this study, the oxidation mechanisms of as-sprayed and heat-treated Cr_3C_2-NiCr blended powder-based coatings are characterized. Interdiffusion between the coating phases with long-term exposure increased the Cr content of the matrix phase. This had a significant effect on the oxidation mechanism. The implications of the change in oxidation mechanism and oxide morphology on the coating response to high-temperature erosion are discussed.

Keywords cermet coatings, corrosion of HVOF coatings, HVOF coatings, HVOF microstructures, thermal and phase stability of coatings

1. Introduction

Cr_3C_2-NiCr coatings are the second most commonly applied thermal spray coatings for wear applications after WC-Co (Ref 1). Their superior oxidation resistance has seen them applied in a range of applications subject to combined erosion and high-temperature corrosion. However, little has been presented regarding the mechanism of degradation in such industrial environments (Ref 2). Under such conditions, oxide scales take on an ever more significant role in determining the wear performance (Ref 3). The oxidation mechanism and kinetics of bulk alloys have been well characterized. However, the situation with regard to thermal spray coatings in general is less understood. Add to this the additional factors of a two-phase structure (carbide grains and the NiCr alloy), in-flight degradation and a generic ''splat''-based morphology, and the oxidation mechanism of Cr_3C_2-NiCr becomes very complex. However, a detailed understanding of this mechanism is required for the future application of such coatings as the requirements of industry push for extended coating lifetimes and reliability at higher operating temperatures and under more aggressive wear conditions.

In this study, the oxidation mechanism of Cr_3C_2-NiCr thermal spray coatings at 700 and 850 °C is presented. The coatings were sprayed using a powder mixture made by ''blending'' pure Cr_3C_2 powder with a Ni20Cr alloy powder. Blended powder-based coatings represent the original microstructure upon which the reputation of this coating composition was built, and are still widely used today. However, the high temperatures at which they are employed leads to changes in their composition and microstructure during extended periods in service (Ref 4, 5). It is important to define these changes and what effect they have on the resulting oxidation mechanism. In this study, blended powder-based coatings were oxidized in the as-sprayed state and after heat treatment at 900 °C for up to 30 days. Heat treatment was used to accelerate the changes that occur with high-temperature exposure and enable the coating to generate a steady-state composition and microstructure. The aim of this study was to develop an understanding of the oxidation mechanism of the coating composition with this simplified coating microstructure prior to developing an oxidation mechanism for the more complex microstructures formed from agglomerated/sintered powders.

2. Experimental Procedure

Coatings were prepared using a powder of mechanically mixed chromium carbide and Ni20Cr powders

This article is an invited paper selected from presentations at the 2009 International Thermal Spray Conference and has been expanded from the original presentation. It is simultaneously published in *Expanding Thermal Spray Performance to New Markets and Applications: Proceedings of the 2009 International Thermal Spray Conference*, Las Vegas, Nevada, USA, May 4-7, 2009, Basil R. Marple, Margaret M. Hyland, Yuk-Chiu Lau, Chang-Jiu Li, Rogerio S. Lima, and Ghislain Montavon, Ed., ASM International, Materials Park, OH, 2009.

S. Matthews, School of Engineering and Advanced Technology, Massey University, Auckland, New Zealand; and **B. James** and **M. Hyland**, Department of Chemical and Materials Engineering, University of Auckland, Auckland, New Zealand. Contact e-mail: s.matthews@massey.ac.nz.

Table 1 Powder production routes and properties

Powder	Manufacturing method	Particle size (μm)	Melting point, °C
Chromium carbide (Cr_3C_2) (WOKA chromium carbide)	Crushed	−45/+5	1811
Ni-20Cr (Sulzer Metco 43VF-NS)	Water atomized	−45/+5	1400

Table 2 Thermal spray system and operating parameters

Spray parameters	HVOF
Spray system	GMA Microjet
Fuel	Propane
Fuel consumption	23.6 L/min
Oxidant	Oxygen
Oxidant consumption	42.5 L/min
Nozzle length	32 mm with 38 mm air-cap
Powder feedrate	11.7 g/min
Carrier gas	Nitrogen
Carrier gas consumption	870 L/h @ 290 kPa
Spray distance	125 mm
Traverse speed	55 mm/s

(Table 1). The powder composition was 75wt.%Cr_3C_2-25wt.%(Ni20Cr). This was sprayed on to grit-blasted mild steel substrates to a thickness in excess of 1 mm by a high-velocity oxygen fuel (HVOF) thermal spray system (GMA Microjet HVOF, General Metal Alloys International, Esneux, Belgium) using the parameters listed in Table 2.

Samples of 15 mm × 15 mm were cut from 100 mm × 50 mm-sprayed mild steel plates for oxidation testing. The substrate was cut off the coating using a metallographic cutting machine. Any remaining steel on the coating was removed by dissolution in hot nitric acid. Compositional analysis indicated that this procedure did not affect the composition or microstructure of the coating (Ref 6).

A number of *coating-only* samples were heat treated at 900 °C in still air for 5 and 30 days, respectively. The as-sprayed and heat-treated coating-only samples were then ground and polished, with a final polishing step using 3 μm diamond abrasive. The grinding process removed all traces of oxide as well as the top layer of material where oxidation may have induced microstructural or compositional changes. This treatment ensured that the as-sprayed and heat-treated microstructures alone were being analyzed, without the possibility of oxidation during heat treatment impacting on the observed response.

Analysis of the coating cross sections was performed using optical microscopy and scanning electron microscopy (SEM) with back scattered electron (BSE) imaging (Philips XL30S-FEG, FEI Company, Hillsboro, OR, USA). Phase analysis of the large flat sample surfaces was performed using locked couple XRD (Bruker D8 Advance, Bruker AXS, Karlsruhe, Germany) (Cu source $K_{\alpha 1} = 1.542$ Å) and energy dispersive spectroscopy (EDS) (EDAX Genesis, Mahwah, NJ, USA).

Table 3 Heat treatment exposure conditions and oxidation conditions

Heat treatment exposure time	5 and 30 days
Heat treatment temperature	900 °C
Heat treatment environment	Still air
Oxidation samples	As-sprayed Heat treated for 5 days Heat treated for 30 days
Oxidation temperature	700 and 850 °C
Oxidation time	10 min, 2 h, and 48 h

Oxidation testing was performed in still air using thermogravimetric analysis (TGA) (Setaram TGA 92, Setaram Instrumentation, Caluire, France). Samples were oxidized for 10 min, 2 h, and 48 h at 700 and 850 °C (Table 3). The oxide morphology was assessed from topographical and fracture specimens examined by SEM. Compositional development of the thin surface oxide was characterized by glancing angle XRD (Bruker D8 Advance, Bruker AXS, Karlsruhe, Germany) (Cu source $K_{\alpha 1} = 1.542$ Å). In locked couple XRD, the most common form of XRD measurement, the x-ray source and the detector are moved together so that the angle that the incident x-ray beam strikes the sample is the same as the angle that the detector collects the x-rays leaving the surface. In contrast, in glancing angle XRD, the x-ray source is held fixed at a low incident angle while the detector is moved through angles of 0 to 90° to detect the diffracted x-rays. The depth of analysis in this technique is shallower than in conventional locked couple XRD and hence it is more sensitive to material on the surface of the sample.

3. Results and Discussion

3.1 Coating Characterization

Figure 1 illustrates the characteristic thermal spray coating microstructure of a blended powder-based coating. In the build-up of long thin ''splats'' of molten material, three phases can be seen: NiCr (the lightest contrast phase, i), chromium carbide (mid gray contrast phase, ii), and an oxide (darkest contrast phase, iii). The carbide and NiCr alloy phases were clearly discernable from each other and did not interact during coating formation.

Rapid solidification of the NiCr splats led to broadening of the XRD spectra peaks due to the small crystal size of this phase. The carbide phase peaks were of low intensity relative to the Ni alloy peaks, despite the dominant nature of this phase in the BSE analysis. While Cr_3C_2 was the dominant carbide phase in the powder, Cr_7C_3 was the dominant carbide phase in the as-sprayed coating. These results indicate that the chromium carbide powder particles underwent significant decarburization during spraying from Cr_3C_2 to Cr_7C_3. The broad nature of the dominant Cr_7C_3 peak in the as-sprayed coating XRD spectrum suggests that the crystal size of this phase as very small. The ''stringers'' of thin oxide were identified as Cr_2O_3.

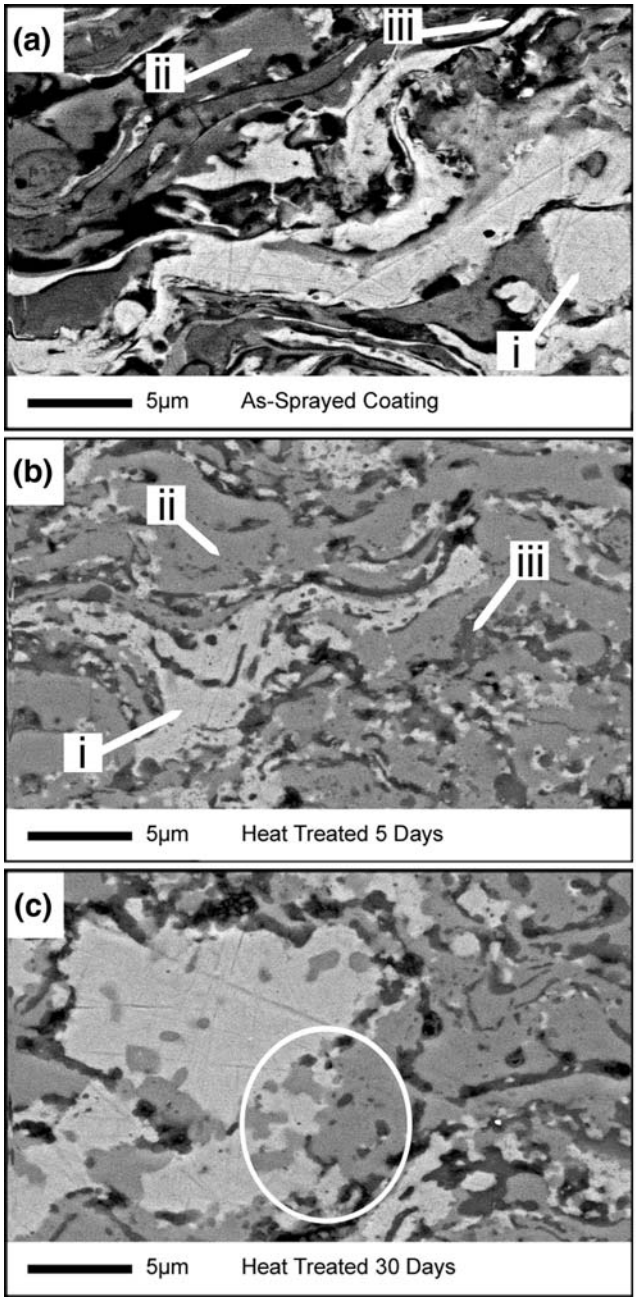

Fig. 1 BSE cross-sectional images of the as-sprayed coating (a) and the coating following heat treatment for 5 days (b) and 30 days (c). Symbols: NiCr alloy (i), chromium carbide (ii), and oxide phase (iii)

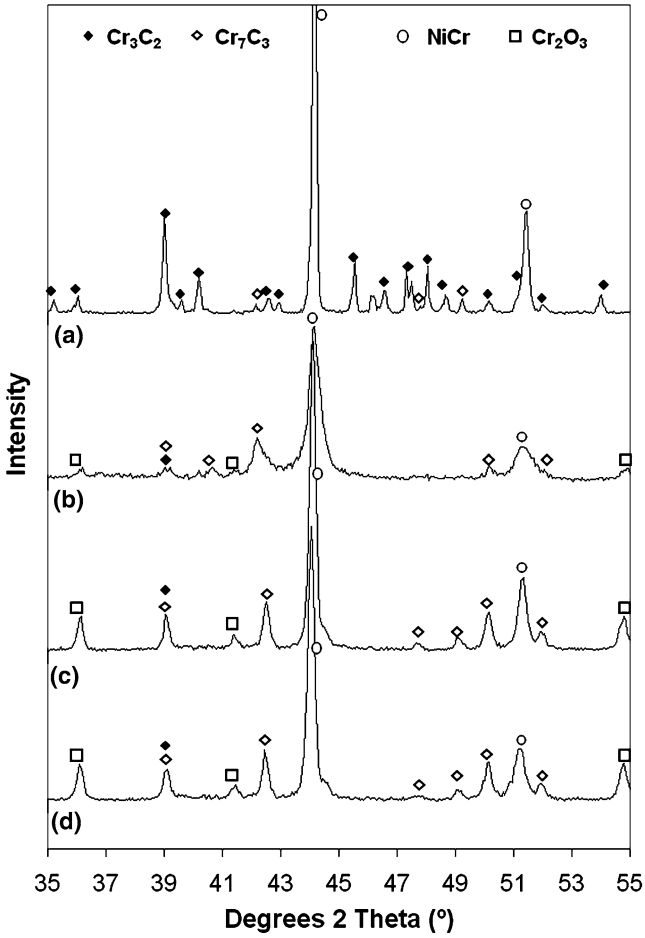

Fig. 2 XRD spectra for the blended powder (a), the as-sprayed coating (b), and the coatings heat treated for 5 days (c) and 30 days (d)

Rapid phase development occurred within the first 5 days of heat treatment, after which minimal changes occurred out to 30 days exposure (Fig. 1). Extensive internal intersplat Cr_2O_3 development occurred between the splats and in zones of porosity by diffusion of oxygen along the splat boundaries into the interior of the coating (Fig. 1, 2). Heat treatment led to intersplat sintering and the disappearance of the splat boundaries. Diffusion of carbide elements into the NiCr alloy regions was implied by the rounded and spherical nature of the carbide grains, and the formation of irregular and nodular interfaces along the previously smooth carbide-NiCr splat boundaries is indicated in Fig. 1(c). This resulted in the increase in the Cr content of the NiCr alloy splats as detected by EDS. Care was taken to analyze regions in the middle of large splats to avoid the inclusion of neighboring carbide splats in the volume of analysis. Chromium concentrations in excess of 26 wt.% in the center of large alloy splats suggest that the Cr content in the zones closer to the carbide phases would be even higher. To assess the thermodynamic feasibility of this observation, calculations were performed using the software package HSC Chemistry (Ref 7). Based on the assumption of total decarburization from Cr_3C_2 to Cr_7C_3, as indicated by XRD, the overall molar concentrations of Cr, C, and Ni are predicted to form a Ni alloy with 31 wt.% Cr at 900 °C. Hence, it is reasonable to expect an increase in the Ni alloy Cr content with long-term exposure at 900 °C from a phase equilibrium viewpoint.

Cr_7C_3 was the only carbide phase detected by XRD out to 30 days of heat treatment. These results suggest that the Cr_7C_3 phase in this study was formed by decarburization during spraying, rather than as a result of decarburization during heat treatment. Rapid solidification of this molten phase during coating formation resulted in very low-intensity XRD peaks. With heat treatment, the Cr_7C_3 phase recrystallized and was able to be detected by XRD (Fig. 2). Vlasyuk et al. (Ref 8, 9) reported a similar stable carbide composition while treating Cr_3C_2-NiCr composites up to 900 °C. Taylor (Ref 10) observed variable results during heat treatment of Cr_3C_2-based blended powder plasma and D-Gun coatings. The shrouded plasma spray process generated minimal in-flight carbide degradation. Heat treatment of the coating at 1021 °C for 100 h generated minimal carbide phase decomposition and no significant increase in the Cr_7C_3 concentration. In contrast, significant in-flight carbide degradation from Cr_3C_2 to Cr_7C_3 occurred in the D-Gun coating. With heat treatment, the Cr_7C_3 content continued to increase, becoming the dominant carbide phase at a treatment temperature of 871 °C. These observations highlight a key issue in chromium carbide degradation during thermal spraying. The high retained Cr_3C_2 content of the plasma coating in Ref 10 and lack of carbide degradation with heat treatment indicates that Cr_7C_3 formation from Cr_3C_2 degradation is not favored over the heat treatment temperature range considered here.

3.2 Oxidation Mechanism at 700 °C

3.2.1 As-Sprayed Coating. At 700 °C, the NiCr and chromium carbide splats oxidized independently of each other according to the oxidation mechanisms presented for bulk materials of Ni20Cr and chromium carbide (Fig. 3a-c).

Chromium carbide splats oxidized by a stepwise decarburization mechanism prior to the formation of Cr_2O_3 (Ref 6, 11, 12).

Equation for the stepwise mechanism of oxidation of Cr_3C_2 is as follows:

$$Cr_3C_2 \overset{+O_2}{\rightarrow} Cr_7C_3 \overset{+O_2}{\rightarrow} Cr_{23}C_6 \overset{+O_2}{\rightarrow} [Cr_{MET}] \overset{+O_2}{\rightarrow} Cr_2O_3 \quad \text{(Eq 1)}$$

This mechanism was reflected in the formation of Cr_7C_3 by oxidation of Cr_3C_2 during thermal spraying. No $Cr_{23}C_6$ was detected by XRD, indicating that this phase must have formed a very thin layer prior to Cr_2O_3 formation (Fig. 4). The phase transitions from Cr_7C_3 to Cr_2O_3 occurred very rapidly at this temperature as evident by the formation of a thin continuous Cr_2O_3 layer after 10 min exposure (Fig. 3a). With extended exposure, the oxide layer thickened. As discussed in Ref 6, carbide oxidation occurs by diffusion of oxygen through the oxide layer down to the oxide-carbide interface. Oxide formation occurs at the oxide-carbide interface by consumption of the carbide phase itself. Unlike in a Cr alloy, Cr atoms in the carbide are locked into the compounds structure and are not free to diffuse out to the gas-oxide interface. In this way, the carbide phase is progressively consumed by the oxidation process.

NiCr oxidation occurred in a manner typical of Ni-20Cr alloys reported in the literature (Ref 13). NiO rapidly nucleated within the first 10 min of exposure (Fig. 4) before being encapsulated from below by the slower growing Cr_2O_3 phase. $NiCr_2O_4$ was formed as a result of the Cr_2O_3 consumption of NiO (Ref 13).

Two different oxide morphologies developed during oxidation of the NiCr splats. On the thin bands of NiCr splats, bulbous NiO rapidly formed. In contrast, the oxide formed on the larger area splats was thinner, but also heterogeneous. Large oxide grains were formed in the center of such regions, while the oxide grains size became significantly smaller in moving toward the splat periphery (Fig. 3a-c).

Dramatic growth of the bulbous oxide features occurred during the first 2 h of exposure (Fig. 3b). EDX analysis indicated that these features were composed of oxides containing Ni. A distinctive feature of these bulbous oxides was that, in spite of extensive vertical growth, the base of such features remained solely on the NiCr alloy phase splat with minimal lateral development over neighboring carbide splats. The mechanism accounting for the relationship between such extensive bulbous NiO growth and the thin bands of exposed NiCr alloy splats is currently unknown. However, the dominance of NiO growth implies a localized reduction in Cr concentration. Factors such as reduction in Cr content through in-flight oxidation, in addition to the long diffusion path of a thin ''pancake''-like splat morphology, may contribute to the observed phenomenon.

The oxide layer formed on the larger area of the NiCr alloy thickened and became more homogeneous with 2 h exposure (Fig. 3b). The finer grained carbide oxide layer remained distinctly thinner than the oxide on the NiCr alloy. With extended exposure, the NiCr oxide began to encroach over the neighboring carbide grains. Such intersplat growth indicates that the neighboring splats were in physical contact, implying that the splat boundaries had been filled to create a physical bond. This may have occurred by sintering, but is more likely to have been dominated by internal oxidation of the coating along the splat boundaries.

NiCr alloy oxide development occurs by outward diffusion of Cr to the oxide-gas interface, while carbide oxidation occurs by inward diffusion of oxygen to the oxide-carbide interface (Fig. 5). As the oxide above the NiCr alloy phase thickens, the rate of Cr supply to the gas-oxide interface is reduced due to the extended diffusion barrier. The shorter diffusion path for the NiCr alloy Cr atoms out over the carbide phase would then favor lateral oxide development. This suggests that NiCr alloy oxide encroachment over the carbide phase occurs by diffusion of NiCr alloy Cr atoms out through the Cr_2O_3 grain boundaries of the carbide oxide to the gas-oxide interface over the carbide grains. Furthermore, lateral development on account of internal oxidation within the surface layer of the NiCr alloy oxide would provide an additional mechanism for encroachment of the NiCr alloy oxide over the neighboring carbide grains.

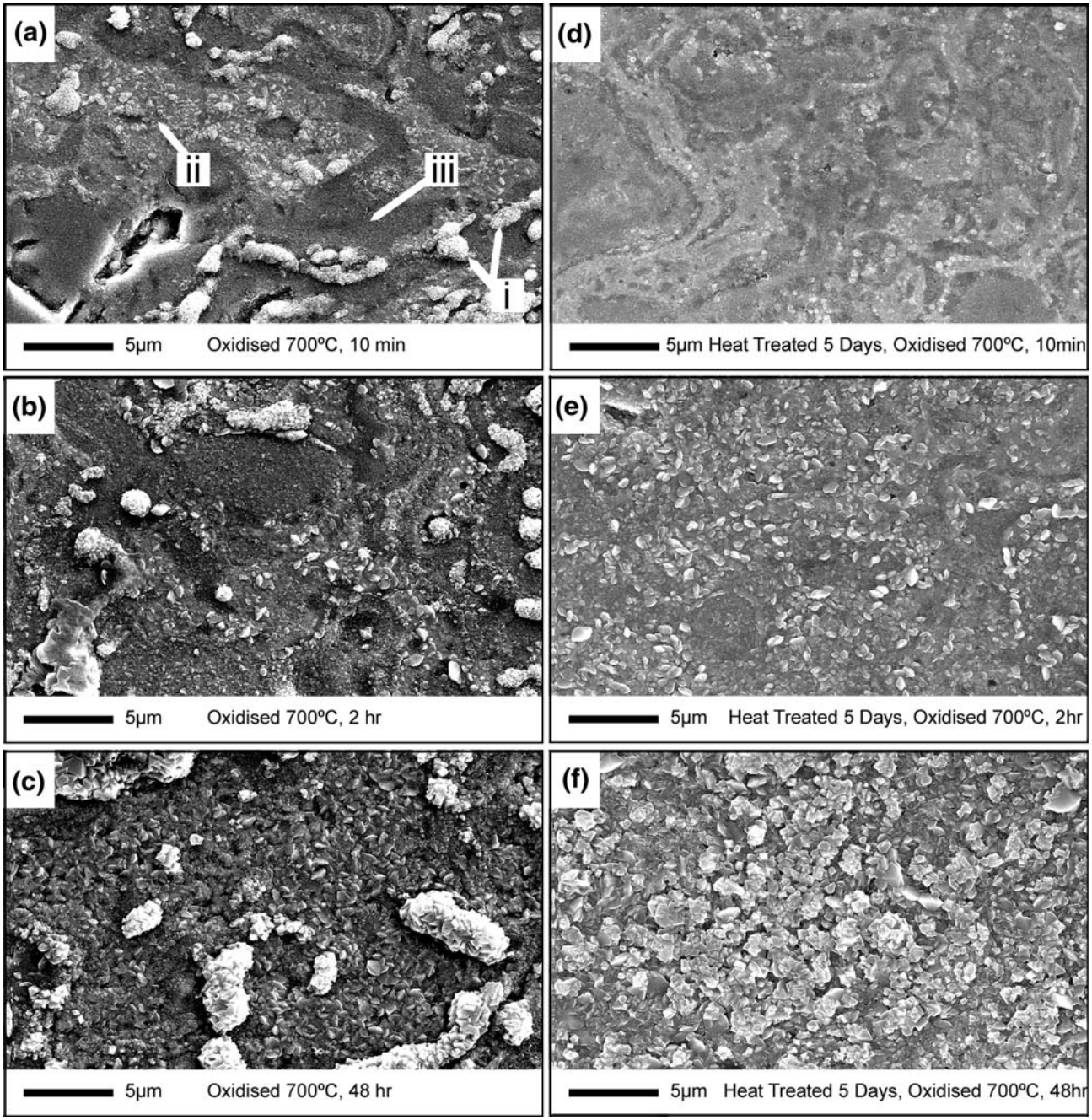

Fig. 3 Surface oxide development on the as-sprayed coatings at 700 °C following 10 min (a), 2 h (b), and 48 h (c) of exposure. This is in contrast with the surface oxide development on the 5 day heat-treated coating oxidized at 700 °C following 10 min (d), 2 h (e), and 48 h (f) of exposure. Symbols: Bulbous NiCr alloy oxide layer (i), Flat NiCr oxide layer (ii), and chromium carbide oxide layer (iii)

3.2.2 Heat-Treated Coating. Sintering of the splats during heat treatment allowed Cr to diffuse from the carbide into the metal alloy. This had a significant effect on the oxidation mechanism of the alloy. Unlike the as-sprayed coating, the oxide on the NiCr alloy was flat, not bulbous after 10 min at 700 °C (Fig. 3d). The carbide phase oxide formed in a similar manner as on the as-sprayed coatings, being thin, flat, and continuous.

With extended exposure, the NiCr-based oxide continued to thicken and lateral growth over the neighboring carbide splats occurred with 48 h exposure (Fig. 3d-f). No bulbous NiO features developed over this time.

Unlike the as-sprayed coating, Cr_2O_3 dominated the oxide composition over the duration of oxidation and very little NiO formed (Fig. 6). The NiO phase was consumed by the solid-state reaction with Cr_2O_3 to form $NiCr_2O_4$

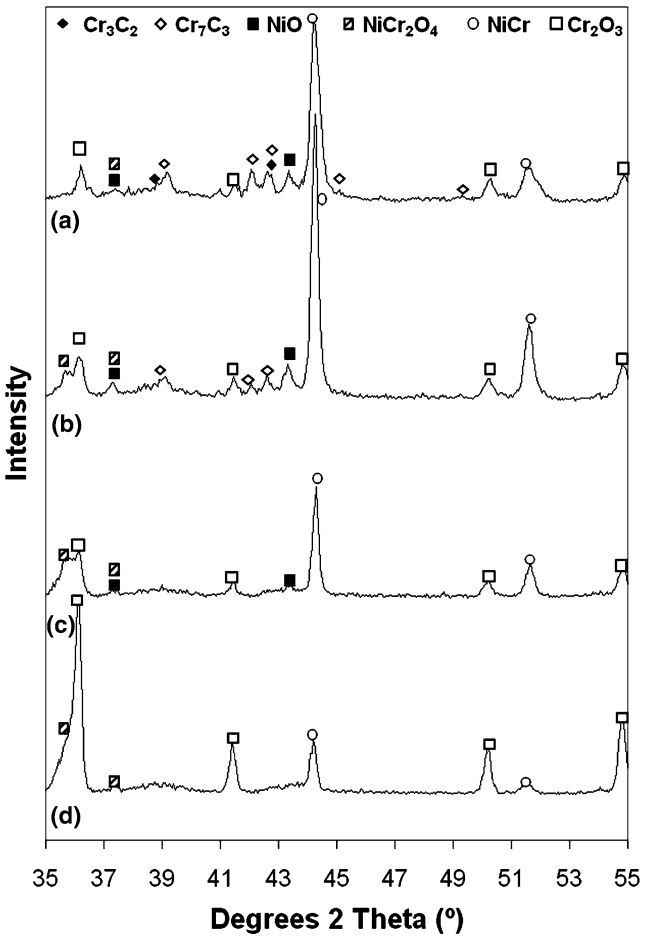

Fig. 4 XRD spectra for the as-sprayed coating oxidized at 700 °C for 10 min (a), 2 h (b), and 48 h (c), and at 850 °C for 48 h (d)

within the 48 h treatment time. The degree of NiO formation was dramatically lower than observed in the as-sprayed coatings due to the higher Cr concentration of this phase resulting from heat treatment. Cr_7C_3 was the only carbide phase observed out to 48 h.

Extended heat treatment for 30 days had no significant influence on the magnitude, morphology, or mechanism of oxide formation.

3.3 Oxidation Mechanism at 850 °C

3.3.1 As-Sprayed Coating. At 850 °C, the same oxidation mechanism occurred as at 700 °C, but at a significantly faster rate (Fig. 7a-c). NiO development was more extensive and occurred over a longer period of time. The bulbous NiO growths were significantly larger than at 700 °C, but again did not develop over the carbide grains. Lateral encroachment was only observed after 48 h, by which time the NiO phase had been consumed by reaction with Cr_2O_3 to form $NiCr_2O_4$. This implies that a continuous Cr_2O_3 sublayer had formed below the Ni-based oxide layer. This in turn would allow lateral Cr_2O_3 formation to

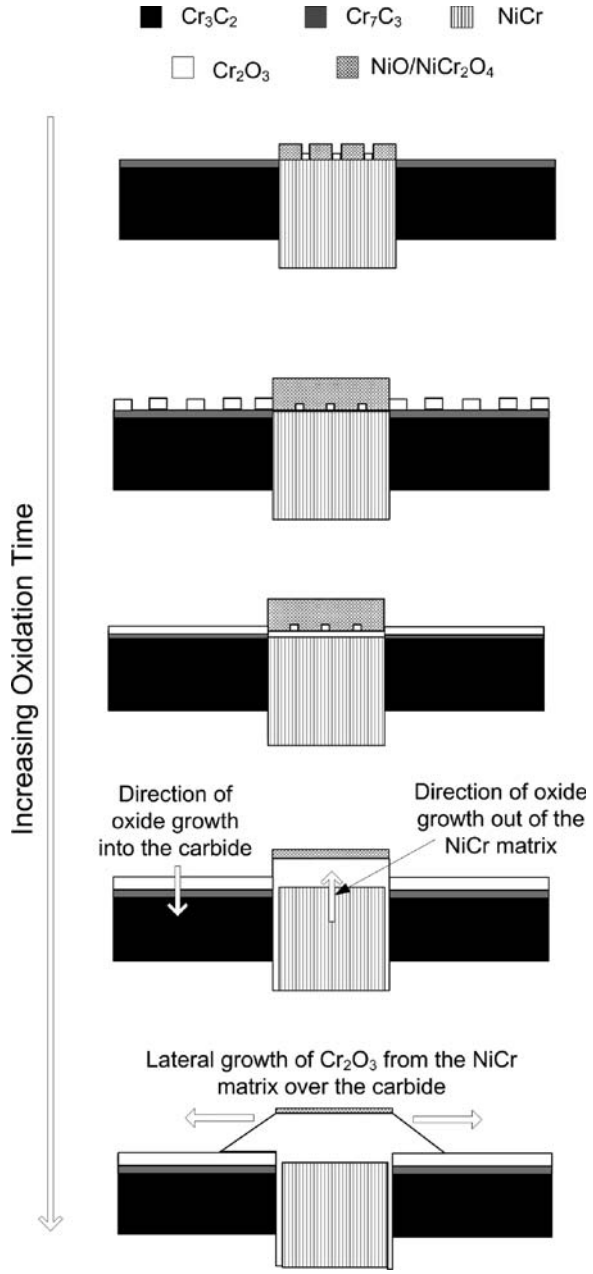

Fig. 5 Schematic illustration of the proposed oxide formation mechanism

occur from beneath such nodular growths out over the carbide by the same mechanism as discussed previously.

3.3.2 Heat-Treated Coating. At 850 °C, the 5 day heat-treated samples oxidized in the same manner as described at 700 °C, but at a faster rate (Fig. 7d-f). The NiCr-based oxide quickly dominated the coating oxide layer, largely overgrowing the carbide-based oxide within the first 2 h of exposure. Such lateral growth continued out to 48 h to such an extent that it became difficult to distinguish the finer grained carbide oxide layers. No bulbous NiO features developed with extended exposure.

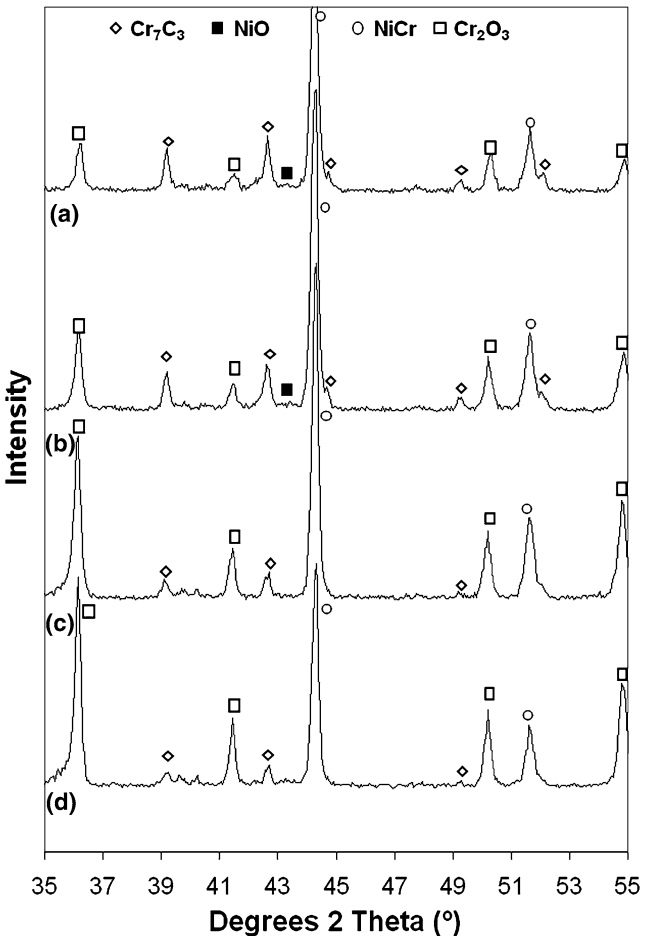

Fig. 6 XRD spectra for the 5 day heat-treated coating oxidized at 700 °C for 10 min (a), 2 h (b), and 48 h (c). XRD spectra for the 30 day heat-treated coating oxidized at 700 °C for 48 h (d)

Cr_2O_3 again dominated the oxide composition (Fig. 6d). Low-intensity features in the XRD spectra indicative of $NiCr_2O_4$ implied some degree of NiO formation within the first 2 h; however, this was very minor. Cr_7C_3 was the only carbide phase detected showing no indication of transformation to $Cr_{23}C_6$.

The extended duration of heat treatment from 5 to 30 days had no obvious effect on the oxidation mechanism. This result indicates that intersplat sintering and diffusion of Cr from the carbide into the alloy occurred well within the first 5 days of heat treatment. Furthermore, sufficient Cr diffusion occurred to significantly suppress the extent of NiO growth. The lack of significant NiO formation and the increase of the Cr content above 26 wt.% with heat treatment in this work support the results of Moulin et al. (Ref 14). Their work indicated that Cr concentrations in excess of 27.5 wt.% in NiCr alloys are required for Cr_2O_3 to totally suppress NiO formation during oxidation.

3.4 Implications for High-Temperature Application

The most significant effect of heat treatment was the increase in the NiCr alloy Cr content which enabled a protective Cr_2O_3 base oxide to form more quickly than in the as-sprayed coating. However, before this conclusion can be applied in practice, it must be considered in the correct context. Heat treatment was performed at 900 °C, the upper limit of applications for Cr_3C_2-NiCr coatings. While the mechanism of microstructural and compositional development are believed to be consistent over the 700 to 850 °C temperature range of interest, it is the *rate* of such development that needs to be considered. The compositional changes with heat treatment were dictated by the temperature-dependent diffusion of Cr and C from the carbide into the NiCr alloy. Cr diffusion will be relatively slow due to its substitutional position in the Ni lattice. Carbon diffusion via interstitial lattice sites can occur significantly faster. Consideration of the relative diffusivities of Cr and C in a Ni matrix indicates that it will take up to 13.5 times as long (Ref 6) for diffusional processes to generate comparable microstructures at 800 °C as were observed at 900 °C in this study. At lower temperatures such diffusional processes are considerably slower.

An additional complication is the effect of temperature on the rate and mechanism of Cr and C separation from the carbide such that they are able to diffuse into the NiCr alloy. Solid-state sintering in Cr_3C_2-Ni composites has been reported at temperatures of 700 to 800 °C by Vlasyuk et al. (Ref 8, 9). Cr atoms were thought to diffuse into the Ni binder, generating a physical bond between the two phases as well as forming a band of low Cr content NiCr alloy around the carbide periphery, which is consistent with the results of this study. Diffusion appeared unidirectional up to 900 °C (Ref 8, 9) with no Ni diffusion into the carbide phase in spite of the increasing degree of Cr alloying in the Ni phase with increasing temperature. In contrast to the work of Vlasyuk et al. (Ref 8, 9), Taylor (Ref 10) hypothesized that it was the C, not Cr, that was the principal diffusion species based on the formation of Cr_7C_3 and $Cr_{23}C_6$ at the grain boundaries within the NiCr splats of Cr_3C_2-NiCr coatings.

Based on these studies, it is evident that, at high temperature, it is the carbide elements that are mobile within the NiCr alloy phase and responsible for the observed variation in composition and microstructure. The mechanism by which Cr and/or C are freed from the carbide is, however, debatable. Each of the above studies highlighted either Cr or C diffusion without detailing specifically the response of the alternate element. While not detected until very high temperatures in the work of Vlasyuk et al. (Ref 8, 9), C must diffuse away from the carbide phase at lower temperatures since Cr_3C_2 is the most C rich of the chromium carbides and hence could not accommodate excess C within the carbide structure as would be required by Cr dissolution alone into the NiCr alloy. It is possible that the excess C was dissolved within the NiCr alloy or incorporated as a fine phase that was not distinguished from the carbide particles. Similarly, the evident alloying of Ni by Cr in the work of Vlasyuk et al. (Ref 8, 9) suggests that it is unlikely that only C diffuses in the work of Taylor (Ref 10). In addition, the complex structures of Cr_3C_2 and Cr_7C_3 highlighted by Guilemany et al. (Ref 15) suggests that it is unlikely that the structure simply reorients itself from that of Cr_3C_2 to Cr_7C_3, as would be

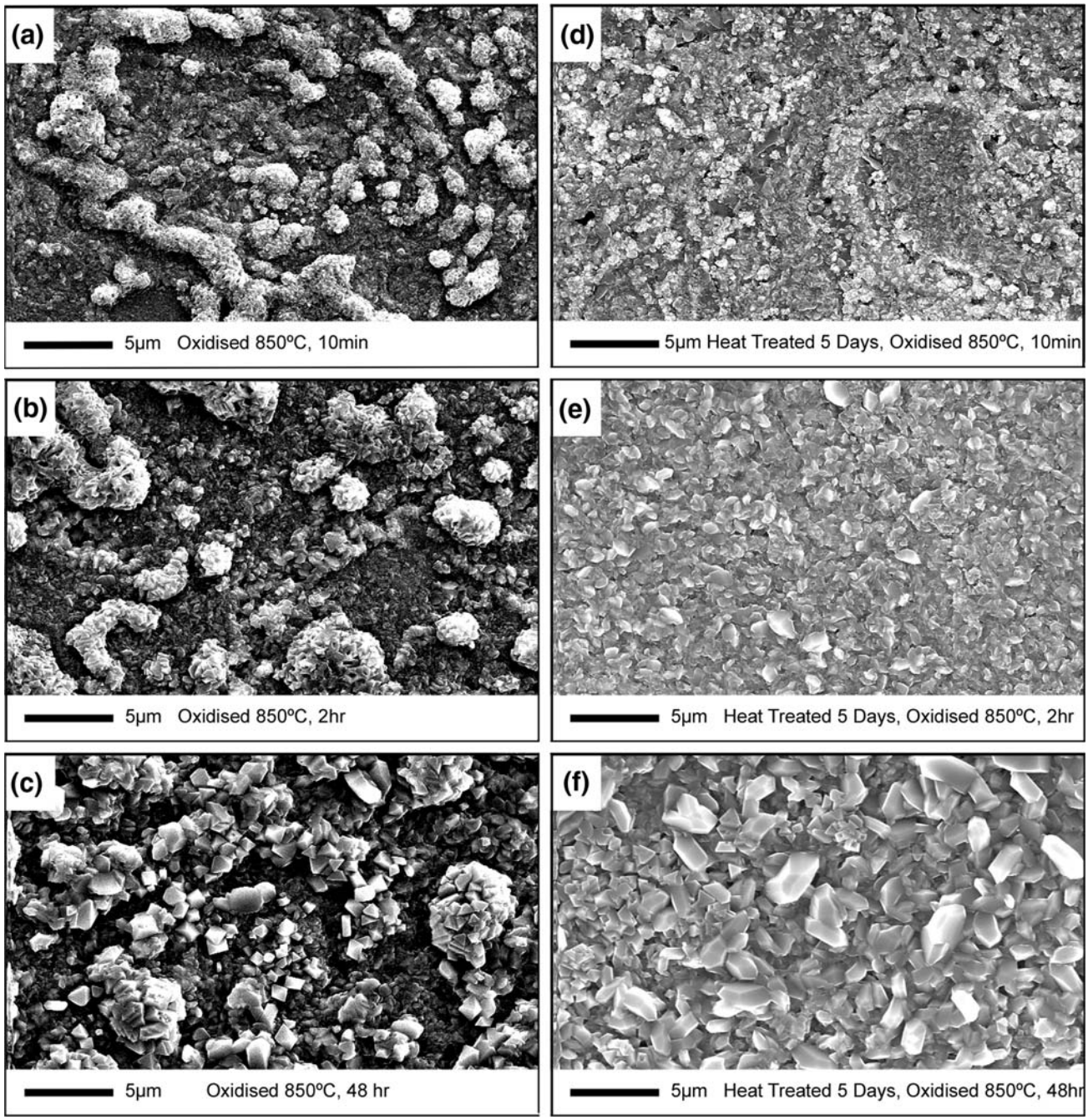

Fig. 7 Surface oxide development on the as-sprayed coatings at 850 °C following 10 min (a), 2 h (b), and 48 h (c) of exposure. This is in contrast with the oxide development on the 5 day heat-treated coating oxidized at 850 °C following 10 min (d), 2 h (e), and 48 h (f) of exposure

required for a C-only diffusion mechanism. In this instance, the excess Cr is likely to have alloyed with the Ni binder phase.

Overall, the results of these literature works, in addition to the observed carbide development in this investigation, indicate that both Cr and C diffuse from the carbide phase into the NiCr alloy phase. Separation of these elements appears to occur by simple dissolution of the individual atoms, in stoichiometric ratios, into the NiCr alloy phase. While Cr released in this manner is accommodated by alloying in the binder phase, the role of C is less clear. This element may be dissolved within the NiCr alloy, may accumulate as graphite at the carbide-NiCr alloy interface, or within the NiCr alloy, or form low-C content carbide phases within the NiCr alloy.

These results indicate that the oxidation mechanism of blended powder-based Cr_3C_2-NiCr coatings will change as a function of long-term in-service exposure; however, the magnitude of this change will be dependent on the exposure temperature. Knowledge of such development in the oxide morphology is particularly significant for Cr_3C_2-NiCr coatings given that they are routinely used as wear resistant coatings at elevated temperatures. As such, the oxide layer formed on the surface plays a direct role in dictating the wear response and the magnitude of long-term corrosive wear. The effect of the oxide morphology on the high-temperature erosion response of these coatings has recently been assessed (Ref 3). The bulbous oxide features formed on the as-sprayed coatings had a positive effect on reducing the magnitude of erodent penetration into the coating. However, the ability of the coating to sustain such a positive oxide morphology with long-term erosion at high temperature was questioned, given the formation of a continuous and flatter Cr_2O_3 subscale. Under certain conditions, preferential erosion of such bulbous features was predicted to accelerate the erosion-oxidation degradation of the coating.

Erosion of the flatter and more continuous Cr_2O_3 scale formed on the heat-treated coating exhibited a more classical erosion response. The erodent penetrated the oxide scale and led to ductile deformation of the underlying Ni alloy phase. The oxide deformed with the underlying alloy phase and remained adherent without signs of spallation under the conditions of testing.

4. Conclusions

This study characterized the variation in the oxidation mechanism of blended powder-based Cr_3C_2-25(Ni20Cr) coatings as a function of heat treatment. The main conclusions drawn from this investigation are:

The as-sprayed coating phases oxidized independently according to the mechanism described for bulk single-phase chromium carbide and Ni20Cr alloy materials. The NiCr alloy rapidly formed NiO which was subsequently consumed by the solid-state reaction with the underlying Cr_2O_3 to form $NiCr_2O_4$. The NiO formed two distinct oxide morphologies: large bulbous oxides on thin regions of exposed alloy and a thinner, flatter oxide layer on the larger area alloy zones.

Heat treatment led to sintering of the splats and diffusion of Cr from the carbide phase into the NiCr alloy. This significantly increased the Cr concentration to the point that it allowed Cr_2O_3 to dominate the oxide composition from the earliest exposure time.

The duration of heat treatment from 5 to 30 days had no effect on the magnitude, morphology, or mechanism of oxide formation at 700 or 850 °C.

Acknowledgments

The authors gratefully acknowledge the assistance of WOKA GmbH, Metal Spray Suppliers (NZ) Ltd, and Holster Engineering (NZ) Ltd for supplying the powder and coatings for this work. The financial assistance provided by Material Performance Technologies (NZ) and The University of Auckland is greatly appreciated.

References

1. L.M. Berger, W. Hermel, P. Vuoristo, T. Mantyla, W. Lengauer, and P. Ettmayer, Structure, Properties and Potentials of WC-Co, Cr_3C_2-NiCr and TiC-Ni Based Hardmetal Like Coatings, *Thermal Spray: Practical Solutions for Engineering Problems*, C.C. Berndt, Ed., ASM International, Materials Park, OH, 1996, p 89-98
2. S. Kamal, R. Jayaganthan, and S. Prakash, High Temperature Oxidation Studies of Detonation-Gun-Sprayed Cr_3C_2-NiCr Coating on Fe- and Ni-Based Superalloys in Air Under Cyclic Oxidation at 900°C, *J. Alloys Compd.*, 2009, **472**(1-2), p 378-389
3. S. Matthews, B. James, and M. Hyland, Erosion of Oxide Scales Formed on Cr_3C_2-NiCr Thermal Spray Coatings, *Corros. Sci.*, 2008, **50**, p 3087-3094
4. S. Matthews, M. Hyland, and B. James, Microhardness Variation in Relation to Carbide Development in Heat Treated Cr_3C_2-NiCr Thermal Spray Coatings, *Acta Mater.*, 2003, **51**(14), p 4267-4277
5. S. Matthews, M. Hyland, and B. James, Long-Term Carbide Development in High Velocity Oxygen Fuel/High Velocity Air Fuel Cr_3C_2-NiCr Coatings Heat Treated at 900°C, *J. Therm. Spray Technol.*, 2004, **13**(4), p 526-536
6. S. Matthews, "Erosion-Corrosion of Cr_3C_2-NiCr High Velocity Thermal Spray Coatings," Doctoral Thesis, Department of Chemical and Materials Engineering, The University of Auckland, Auckland, 2004
7. A. Roine, *HSC Chemistry*, Outokumpo Research Oy, Finland, 1997
8. R.Z. Vlasyuk, I.D. Radomysel'skii, V.P. Smirnov, and A.A. Sotnik, Dissolution of Cr_3C_2 in a Nickel Matrix During Sintering. I: Reaction of Chromium Carbide with Nickel During Solid Phase Sintering, *Sov. Powder Metall. Met. Ceram.*, 1985, **24**(4), p 269-273
9. R.Z. Vlasyuk, I.D. Radomysel'skii, and A.A. Sotnik, Dissolution of Cr_3C_2 in a Nickel Matrix During Sintering. II: Formation of a Liquid Phase in the Cr_3C_2-Ni System During Sintering, *Sov. Powder Metall. Met. Ceram.*, 1985, **24**(5), p 356-360
10. T. Taylor, Phase Stability of Chrome-Carbide NiCr Coatings in Low Oxygen Environments, *J. Vac. Sci. Technol.*, 1975, **12**(4), p 790-794
11. S.F. Korablev, A.V. Lysenko, and S.I. Filipchenko, Chemical and Kinetic Peculiarities of the Oxidation of Powdery Chromium Carbide, *Sov. Powder Metall. Met. Ceram.*, 1988, **27**(7), p 584-587
12. S. Loubiere, C. Laurent, J.P. Bonino, and A. Rousset, Elaboration, Microstructure and Reactivity of Cr_3C_2 Powders of Different Morphology, *Mater. Res. Bull.*, 1995, **30**(12), p 1535-1546
13. N. Birks and G.H. Meier, *Introduction to High Temperature Oxidation of Metals*, Edward Arnold, London, 1983
14. P. Moulin, A.M. Huntz, and P. Lacombe, Influence des Phenomenes Diffusionnels sur le Mechanisme D'Oxydation des Alliages Ni-Cr (Influence of Diffusion on the Mechanism of Oxidation of Ni-Cr), *Acta Metall.*, 1980, **28**, p 745-756
15. J.M. Guilemany and J.A. Calero, Structural Characterisation of Chromium Carbide-Nickel Chromium Coatings Obtained by HVOF-Spraying, *Thermal Spray: A United Forum for Scientific and Technological Advances*, C.C. Berndt, Ed., ASM International, Materials Park, OH, 1997, p 717-721